Journal of Chromatography, 126 (1976) 347–368

CHROM. 9361

NEW MINI-COMPUTER AUTOMATED LINEAR PHOTODIODE ARRAY SPECTROMETER SYSTEM FOR HIGH-RESOLUTION LIQUID CHROMATOGRAPHY

R. E. DESSY

Department of Chemistry, Virginia Polytechnic Institute and State University, Blacksburg, Va. 24061 (U.S.A.)

W. D. REYNOLDS*

Food and Drug Administration, National Center for Toxicological Research, Jefferson, Ark. 72079 (U.S.A.)

W. G. NUNN and C. A. TITUS

Department of Chemistry, Virginia Polytechnic Institute and State University, Blacksburg, Va. 24061 (U.S.A.)

and

G. F. MOLER

Food and Drug Administration, National Center for Toxicological Research, Jefferson, Ark. 72079 (U.S.A.)

SUMMARY

A third generation multi-wavelength array spectrometer was developed as a detector for the high-resolution liquid chromatographic characterization of metabolites. The design features include a PDP-8/e mini-computer, a matched pair of linear photodiode (256 element) arrays (Reticon), holographically ruled gratings, fiber optics, flow cells, and a high-intensity xenon light source. The wavelength range is 256 nm differential with 1 nm resolution and can be independently adjusted in the spectral range of 200–800 nm. Correction for the quantum efficiency curve is made on both of the cooled (−30°) photodiode arrays by an assembly language subroutine. The system is capable of 20 spectra/sec (200–456 nm) in a dual-beam mode. The dynamic range and linearity of the photodiode arrays are approximately 4000:1. Special features include mini-computer driven signal enhancement via integration as a function of signal strength. The display output includes presentation of the total absorption chromatogram *vs.* elution time in both real and post-run time as well as selectable single absorption band (*e.g.*, 280 nm) *vs.* elution time (post-run time). Application of this dedicated mini-computer automated liquid chromatography–UV spectrometry system for the separation and characterization of the metabolites of a carcinogen, 4-ethylsulfonyl-1-naphthalenesulfonamide, will be discussed.

* Author to whom reprint requests should be addressed.

INTRODUCTION

Over the past few years, considerable effort has been expended on developing and improving UV detectors for high-speed liquid chromatographic (LC) separations of biochemically important components[1–14]. Generally, the UV detectors can be divided into two classes which are identified with their end-use, *i.e.*, monitoring *vs.* identification[4]. For general monitoring purposes, most liquid chromatographs successfully utilize a single-wavelength (element) detector at 254 or 280 nm[12]. Other discrete element monitoring has been utilized depending upon the specific sought-for component[8]. For qualitative identification needs, full UV scanning on each component in the LC effluent yields additional spectroscopic information.

Although many varieties of rapid scanning spectrometer systems are available, the *first* generation units relied on moving mechanical parts to scan the spectrum[12,14]. The *second* generation instruments utilized the Vidicon tubes, which eliminated the construction and maintenance problems associated with rotating mirrors or vibrating galvanometers[15,16]. But, the Vidicons suffer from substantial coherent pattern noise, limited integration time due to high dark current as well as memory effects[17,18]. The recent availability of inexpensive solid-state linear photodiode arrays (Reticons) as simultaneous wavelength detectors has enabled the development of *third* generation spectrometers for use in LC[19].

The attainment of rapid-scan UV spectra generates several advantages beyond simple component identification. These advantages occur in several ways, including both time and spectral domains[12–21]. The time–domain advantage accrues in a straightforward manner from the simultaneous detection of the total UV spectra[20,21]. The simultaneous detection of all dispersed radiation (N spectral or spatial resolved elements) reduces the observation time by a factor of N in the case of signal-to-noise ratio (SNR) limited measurements and improves the SNR by a factor of $\sqrt{N}$ for a fixed observation time as in the case of finite LC peak widths. However, further improvements in spectral data (SNR) based on the Hadamard or Fourier methods are limited, at best, for UV spectroscopy, in which the noise is statistical and source dependent[17,20].

In the rapid-scan spectral domain, an improvement in detection level is gained by virtue of the total UV spectrum. By summing the output intensity over all discrete 1-nm channels from 200–350 nm as a single output intensity, an advantage is gained over select single-channel (254 nm) detectability[19]. This increase in detectability (F) varies from component to component but is dependent on the ratio of the integrated area under the spectral curve (200–350 nm) to that at the selected single channel (250 nm). Thus

$$F = \frac{\int_{200}^{350} A\,d\lambda}{\int_{250}^{251} A\,d\lambda}$$

In most cases, this can account for an increase in factors of 5–500 in detectability. For high-speed LC biochemical separations with limited sample size or trace-level components (hormones) in complex physiological mixtures (urine), this improvement would be a decided advantage[22].

Along with the expanding use and development of pesticides, herbicides, food additives, plasticizers, and other environmental chemicals, there has been a growing concern for possible untoward effects of these chemicals in man. Long-term, low-dose feeding effects and related mechanism studies of a few of these agents and model compounds are under study at this Center. Complete studies including identification and monitoring of these agents and their metabolites can be highly informative regarding the activity of the agent, the toxicity and the mechanism of action. High-resolution anion-exchange LC is an excellent analytical tool for studies of this kind because both unconjugated and conjugated metabolites can be separated for structural determination in a single sample without the need for hydrolysis or extensive sample pretreatment. A number of investigators have utilized the anion-exchange column for good separation of diphenylhydantoin and its metabolites, of the glucuronide and sulfate conjugates of *p*-nitrophenol, and of *p*-hydroxyacetanilide metabolites as well as of acetaminophen and its metabolites in human urine[23–25]. Two recent books summarize the application of ion-exchange LC methods to problems in biochemistry and biology[26,27].

This report outlines the development of a minicomputerized linear photodiode array spectrometer system for use as a detector for high-resolution ion-exchange LC. Application of this automated LC–UV system to the separation and characterization of conjugates of 4-ethylsulfonyl-1-naphthalenesulfonamide (ENS) in the urine of BALB/C mice is demonstrated.

INSTRUMENT

General

A proto-type system consisting of a Reticon detector, a light source, optics and a micro-processor was previously constructed by this group[19]. It was determined from this earlier version that certain improvements in system configuration would need to be made in order to develop a system for the high-resolution anion exchange LC separation, UV characterization and identification of metabolic products in urine. Even with maximum external hardware support, the micro-processor limitations in math (data handling, transfer, reduction) and plotting (formatting, I/O) would have to be overcome; and, the spectrometer hardware would also need to be revised for the new design objective. Specifically, the requirements for this type of dedicated minicomputer automated LC–UV system are as follows:

(1) The LC detector system would need to include dual-beam spectrometer operation to accommodate gradient elution.

(2) The system must be capable of taking about 25 spectra/sec to accommodate ensemble averaging (if required).

(3) The spectrum must be in the 200–450 nm range.

(4) Because of the need to quantify the results, the system must be capable of operation in the absorption mode.

(5) The UV source and the electronics must be stable over long periods since a typical LC run utilizing an ion-exchange column would involve a maximum of 80 h and produce nearly 250 peaks.

(6) Due to the large expected volume of data (2.5 million bits/run), all meaningful RAW spectral data must be stored on disk for limited post-run appraisal and then

transferred to industry compatible tape for storage or transfer to the central computing facility. There it would be subjected to various in-depth data reduction programs.

(7) The output format should include total integrated absorption at all measured wavelengths *vs.* elution time (real-time LC) and selectable single-band wavelengths *vs.* elution time as well as individual spectra.

(8) For data handling and reduction, a mini-computer with 12K core and a teletype, a disk, a scope, a magnetic tape and plotter I/O devices will be required.

Although it was fully expected that the ultimate use of such a system might see these stringent requirements relax against long-term needs, the exploration stage would involve a period when it was not known which wavelengths (200–450 nm) were of most importance to the metabolite characterization research. It might be necessary to rescreen previous runs many times to finally focus on the observations which would be used in component identification or for routine monitoring.

The present automated LC–UV system consists of several major units including the high-resolution liquid chromatograph with associated electro-mechanical and electronic controls, a 12-bit computer unit based around a PDP-8/e CPU with 12K of memory and with four interactive storage and display devices, and a spectrometer unit consisting of a xenon light source, fiber optics, and a pair of holographically ruled gratings along with two cooled (−30°) photodiode arrays. Each major unit is discussed in the following sections.

Liquid chromatograph

A high-resolution liquid chromatographic unit utilizing the 150–200 cm ion-exchange columns similar to that developed by Scott was fabricated with some additions and changes[28]. Figs. 1 and 2 are photos of the completed unit. A pH gradient section was added which develops a descending hyperbolic pH gradient (8 → 4.40) during the first 5 h of the 60-h LC run. The system is gradient programmable in five separate inter-dependent functions. The five functions control the two separate gradient development cycles and a final wash cycle as well as start and stand-by modes. The pH buffer gradients are developed from two source solution reservoirs, an initial mixing vessel solution and wash reservoir. The mixing vessel starting solution contains 0.1 *M* buffer (ammonium acetate–acetic acid) adjusted to pH 8 while the other two source reservoirs contain "acid solution" (pH 4.0; 3 *M* buffer) and "buffer solution" (pH 4.40; 6 *M*), respectively. The mixing vessel (stirred) is fed from the three reservoirs through three separate solenoid valves and a mixing vessel feeder pump (two pre-set speeds). A sequence of mixing steps is pre-determined by the operation of the timers and pump speed control. Any combination of curve/linear gradients can be set by this operation. For example, a descending pH gradient can be overlayed on a slow rising linear buffer gradient. A typical operation of the timer sequence is as follows:

(1) The counter/timers are automatically reset upon injection with movement of the injection lever from load to inject (Waters UK6, 6000 p.s.i. injector).

(2) The counter/timers start to count down from their various pre-set points at the rate of one count each minute.

(3) The first counter/timer reaches 0000, which determines the end of the first function and a solenoid valve is switched.

(4) Each successive counter/time in turn continues to count down to 0000 from its individual pre-set point for each designated function.

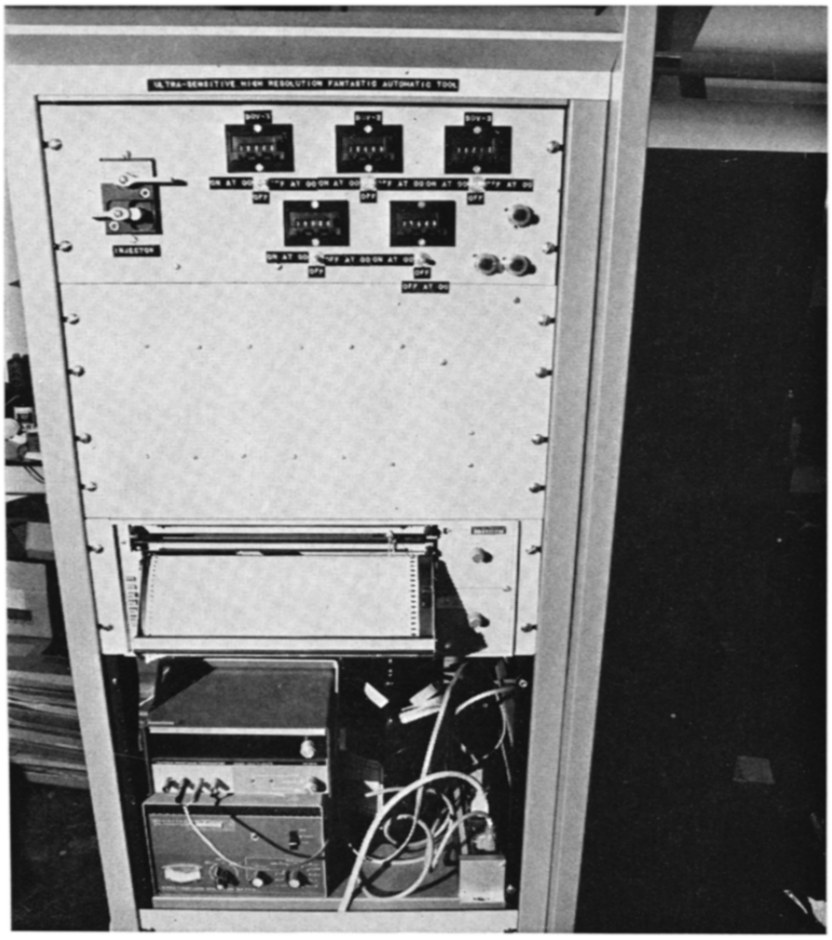

Fig. 1. High-resolution liquid chromatograph utilizing a 150-cm anion-exchange column. Front view.

(5) As the last counter/timer reaches 0000, END OF PROGRAM, the feed pump comes on and pumps the initial solution into the mixing vessel until the level-sensor shuts off the feed pump —END OF RUN (column purged). The column has now been cycled to start the gradient again for another sample.

All materials of construction contacting the sample and eluent are 316 stainless steel, glass or PTFE.

Several different columns (75, 100, 150 cm × 1/8 in. O.D. have) been utilized for the determination of the optimum separation of components in the urine of BALB/C mice. Various anion-exchange resins and particle sizes from several manufacturers have been utilized. Aminex A-27, average particle diameter 13.5 μm (BioRad Labs., Richmond, Calif., U.S.A.), was used with fair resolution but with high ΔP (5000 p.s.i. for 8 M buffer). Another Aminex resin (1-X8L: 9160) of smaller size (6.5 $\pm$ 1.5 μm measured) was used in the 75-cm column with excellent resolution but the ΔP was excessive ($\approx$6200 p.s.i.) at 0.07 ml/min. However, the Aminex A-27 (13.5 μm, 150-cm column; see also Application) appeared to be the best compromise

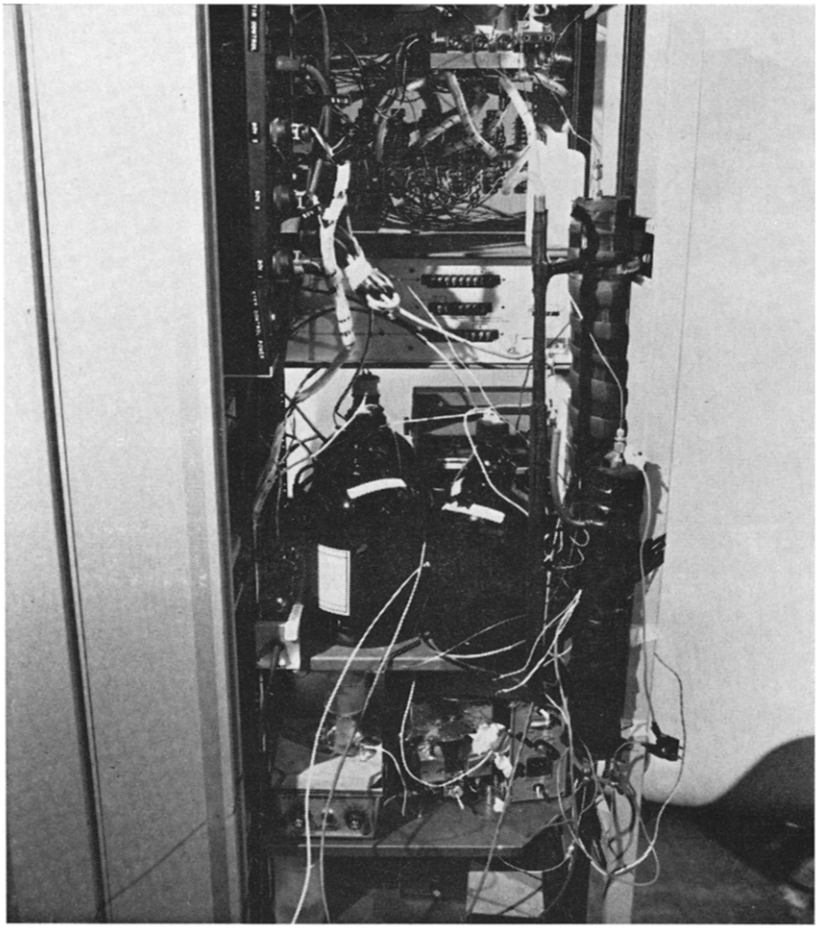

Fig. 2. High-resolution liquid chromatograph utilizing 150-cm anion-exchange column. Rear view.

between flow-rate (elution time), pressure drop, and resolution of the large numbers of urinary components from the conjugates of the model compound, ENS. An example of the separation of both the conjugates of ^{14}C-labeled ENS and urinary components is shown in Fig. 3.

Reticon spectrometer

Light source. A high-intensity 150 W xenon arc lamp and housing with regulated power supply was utilized for the UV source (Model 7301, Oriel Corp.). A fairly smooth continuum output develops from 190–750 nm, as seen in the typical spectral output curve (Fig. 4). The source size is 0.5 × 2.2 mm while the image size at the focal point (76 mm from housing) is 0.9 × 4.0 mm.

Flow-cell. The micro flow-cells, one each for the reference and sample beams, were fabricated in the standard "Z" pattern. The dimensions chosen were dependent both on the size of the available light beam from the fiber optics and the optimum

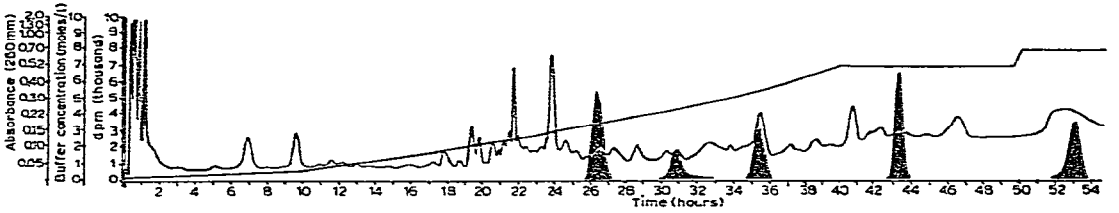

Fig. 3. High-resolution liquid chromatogram of the urine of BALB/C mice (100 μl) containing ^{14}C-labeled ENS metabolites (cross-hatch) and UV urinary components (260 nm).

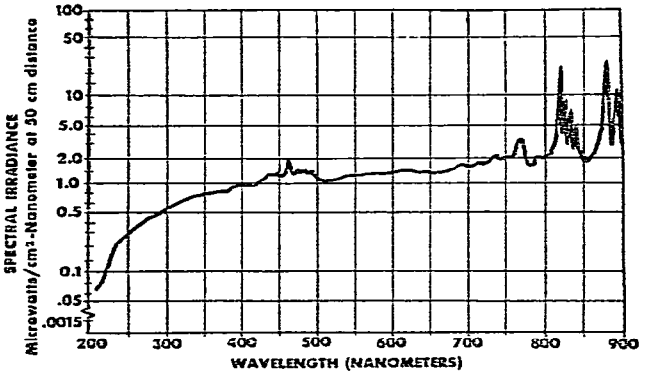

Fig. 4. Spectral irradiance curve *vs.* wavelength of 150 W xenon source.

absorption path-to-volume ratio (1 cm/31 μl) for chromatographic band-width. These flow cells were made from stainless steel with quartz windows and PTFE gaskets.

Grating. The necessity of attaining sub-nanogram sensitivity required a system with best available optics. A high-quality holographically ruled concave grating (600 lines/mm) was used (Model 3B, Jobin-Yvon Optical Systems). This minimized spherical aberration problems as well as keeping reflection and transmission losses to a minimum[15].

Optical path and sensitivity. A metal housing with flat black interior that was also light-tight and purgeable (nitrogen) was fabricated for the optics system. All external entrances and exits were made to minimize light leakage. An optical configuration based on a Rowland circle (F/3.0, 200 mm) as shown in Fig. 5 was placed inside this housing. Use of the grating and fiber-optic bundles reduced the component count over that of other systems, *e.g.*, Czerny–Turner, and hence transmission and reflection losses. The fiber-optics bundle further reduced the alignment problem, so that

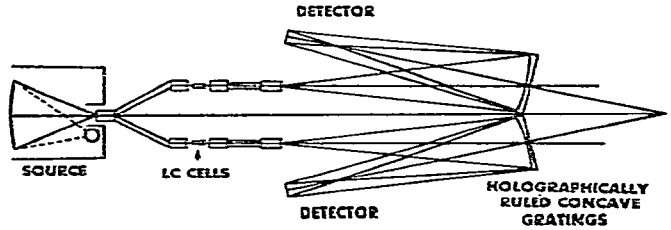

Fig. 5. Optical path including LC flow cells for photodiode array spectrometer.

the system could run for long time periods without recalibration. The overall system involved an F/3.0 rather than the earlier proto-type of F/4.5[19].

Design and optimized performance calculations were completed on the optical system from the light source to signal read-out. These are summarized in Appendices I, II and III. The maximum dynamic range of the linear array (average pixel) was calculated to be 4×10^4:1 (Appendix I). Theoretical design calculations of source strength and sensitivity indicated that with an LC effluent sample containing guanosine ($\varepsilon_{250} = 11{,}050$) and an estimated peak width of 3 min (31 μl cell volume), 1 ng could be detected (Appendices I and II).

Reticon detector. The silicon photodiode linear array detector utilizes a reverse biased p–n junction diode as the photosensitive element. These linear arrays are available in several pixel*/array sizes and pixel areas. Currently, arrays can be obtained with 128–1024 pixels/array with pixel areas of either 1×25 μm or 1×425 μm. These linear arrays are sensitive from below 200 to above 900 nm. They are most efficient in the 600–820 nm region as seen in the typical photon efficiency curve (Fig. 6). Correction for the quantum efficiency curve to a maximum value of 1.0 is made via an assembly language sub-routine before data storage.

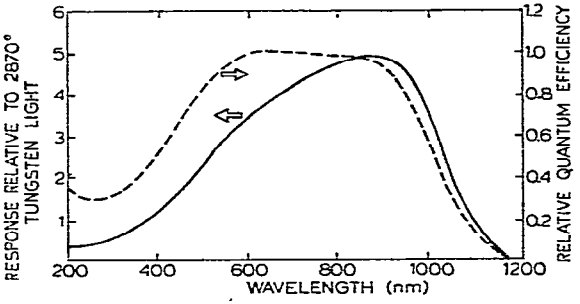

Fig. 6. Quantum efficiency response *vs.* wavelength of the photodiode array (Reticon).

Since the wavelength region of interest for the present instrument was 200–400 nm, a 256-linear array was selected which would enable 1 nm resolution (25 μm centers) with a 256 nm range (200–456 nm). However, this range could be adjusted to any 256 nm band in the 200–900 nm region. Two matched arrays which are individually housed with Pelletier cooling plates (—30°) were selected based on their identical energy response (Model RL256 EC/17, Reticon). Cooling to a —30° aids in the reduction of noise since the noise is reduced by a factor of 2 for each 10° lowering of temperature[17]. A 256-linear array Reticon with a printed circuit background is illustrated in Fig. 7. A schematic of the linear array is shown in Fig. 8. The operation of the photodiode array occurs as follows:

(1) As light strikes the surface of the detector, hole pairs are created and migration occurs toward the capacitor element (Fig. 8).

(2) As the light continues to strike the detector surface this action leads to a gradual discharge of the capacitor.

* A pixel is a simple photodiode and, in the present design, it receives the light from a single wavelength band.

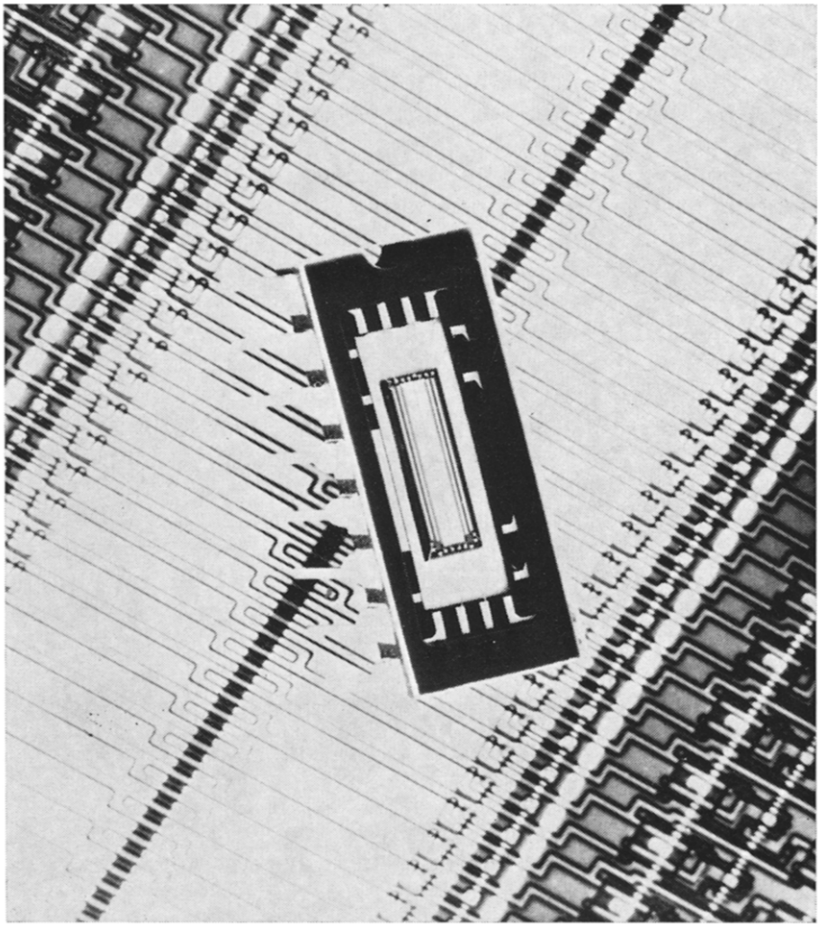

Fig. 7. Photodiode linear array (256 pixel) with printed circuit background.

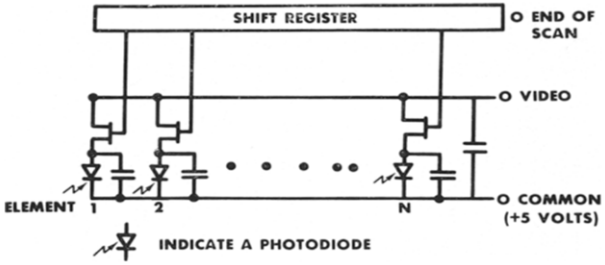

Fig. 8. Schematic of photodiode linear array. Operational view.

(3) Over the integration time (light impact time), the charge on the capacitor drops an amount equivalent to the amount of integrated light following on the detector.

(4) When the pixel is "read", a multiplexer attaches the detector to a voltage source which charges the capacitor back up to a standard potential.

(5) A signal, corresponding to the current-flow necessary to recharge the voltage source, is sent down a wire (video-line).

(6) The multiplexer then causes the voltage source to be switched to the next pixel in the detector, and the process is repeated.

Reticon "read-out". In the fast scanning environment of high-resolution LC operation, continuous monitoring of the photodiode array is unnecessary. 1000 spectra/sec provides more data than can be either stored or handled by a dedicated computer. In practice, it is normal to initiate data collection only periodically. The concepts involved are as follows: During a dead period, when the detector is not being used, the light striking the surface of the detector rapidly leads to saturation of all elements. (See Appendix I for "saturation exposure".) In order to prepare for gathering of spectral information, the array must be "dummy read". This is accomplished by applying a read pulse which starts the drive electronics, and all elements in the array are recharged back to their starting charge points. The *j*th element in the array is read-out at a different time than the *z*th element. However, the time interval between the reading out of the *j*th element in successive scans (integrate or "dwell time") is the same for successively read *z*th elements. Since the "rippling" through elements is fast compared to the LC effluent concentration changes being observed, a truly simultaneous multi-wavelength detector is involved. Consequently, each individual element is continually "on" except for a very short "blink" out of each cycle which can yield a duty time as high as 95%.

If one views the single vidio-line output of the device, a series of pulses appear, each corresponding to the amount of light striking the element of the array that the pulse represents (Fig. 9). These arrays operate with the multiplexer switching between elements at a clock rate of 1 KHz to slightly above 1 MHz. A complete reading of the array (256 pixels) can be as fast as 12 msec to a slower speed of 0.25 sec. The integrate time can be altered between the limits of the Reticon "shift out" rate (20 KHz) and that time when the dark current noise becomes a serious problem. This places a upper limit of 80 spectra/sec to a lower unit of 1 spectra/1000 sec (4 sec/pixel) for the cooled (−30°) array. For optimum integration time, a rate of 20 spectra/sec was chosen.

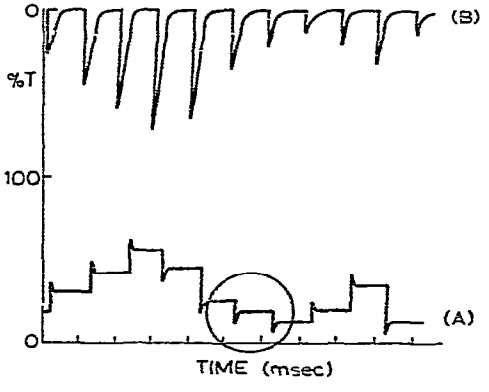

Fig. 9. (A) Time base response of a single pixel to varying light intensity. (B) Video line pulse signal to the single pixel capacitor.

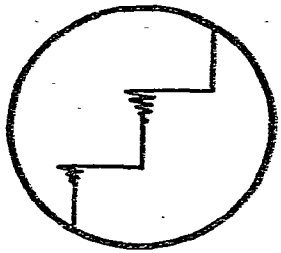

Fig. 10. Typical switching transients developed during a single pixel read-out.

In order to properly condition the serial pulse train exiting from the common video-line of the detector for input to a computer system, it is normal to run it through an amplifier, integrate, sample/hold system with high rejection of periodic noise. The majority of the noise in the detector arises from switching transients induced at times shown in Figs. 9 and 10. This noise can be decreased by careful amplifier design and separation of the clock drive circuitry from the detector itself. Each pulse is integrated over a major fraction of its width, which leads to a reduction in noise by the analog integration operation. A schematic of the detector and amplifiers for both "real time" recording output (integrator) and mini-computer data acquisition (absorbance, transmittance) is shown in Fig. 11. The integrator sums the absorbance signal over all measured wavelengths (200–450 nm) for a given set of "scans".

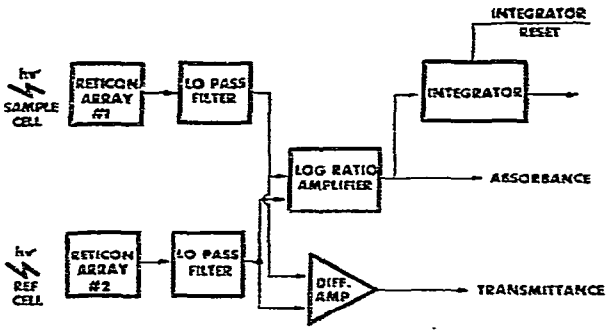

Fig. 11. Schematic of Reticon array detectors (sample, reference) and analog "front-end" for computer input.

Computer

General. The basic computer configuration used to acquire, process, and display the formatted spectral data is based around a 12-bit mini-computer, PDP 8/e (Digital Equipment Corp.) with 12K words of core memory. Additional bus-bar hardware components include a 10-bit A/D convertor (AD8A; D.E. Corp.), a real time clock (DK8E-P; D. E. Corp.), a 10 Hz dayclock, a D/A convertor (VC-8E point plot; D.E. Corp.), and a hardware multiply/divide processor (KE8E; D.E. Corp.). The storage devices include two 3.2 million word disk and controller units (RK8E; D. E. Corp.) and a 9-track magnetic tape (TU-10; D. E. Corp.). The I/O devices include a multi-speed alpha/numeric terminal (LA-36; D.E. Corp.), an incremental plotter

(Cal-Comp No. 565; Cal-Comp Corp.) with interface (XY8E; D.E. Corp.) and display oscilloscope (No. 5051; Tektronix Corp.). A configuration diagram of the computer system is shown in Fig. 12.

Operation. The CPU uses a 10-bit A/D convertor to change the incoming analog signal from the detector to digital which is stored in a 4K word input buffer in the CPU. The data input rate is controlled by two separate clocks. The first real time clock is used to control the integration or exposure time of the Reticon array. The second clock is used as a day clock which is started when an LC run is initiated. This clock is read each time a spectrum is taken, which allows data to be taken only when there is a signal above the baseline. If the response in the reference beam falls below a certain level, the integrate time is increased in binary progression. This is an operation corresponding to slit opening on a regular spectrometer, but without loss in resolution. The integrate time (a 2-bit number) and the output of the A/D (a 10-bit number) are ANDED to provide a 12-bit data point for each pixel in the array, yielding a dynamic range of 1000:1.

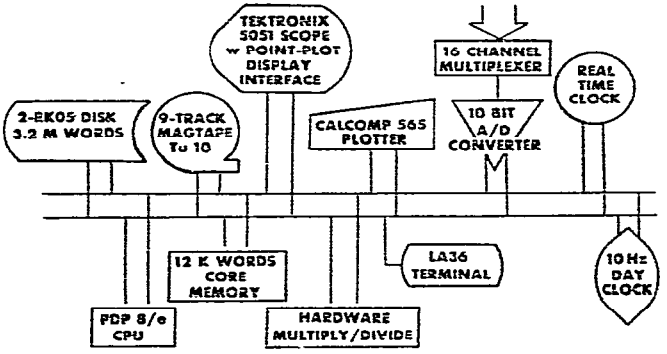

Fig. 12. Mini-computer configuration with I/O devices.

The three data modes (absorbance, transmittance or integral) are carried by the analog multiplexer, which acts as a front-end to the A/D convertor. The data are collected in ping pong double buffers. As each buffer is filled, it is transferred to the disks using assembler drivers that are interrupt oriented. By using this type of rotating buffer for data storage, the possibility of missing incoming data is small. The data are stored on disk in single-word binary formatted files.

The analog amplifiers (front-end) performed all the correction functions except the one for responsivity of the Reticon array (see Fig. 6). This calibration function is accomplished in the computer by ADDING the appropriate correction factor stored in memory for each wavelength as a LOG. The addition function is much faster than other math operations since data through-put is at a premium for ensemble averaging.

Software. A series of software routines were written in various levels of computer languages (assembler, Basic and Fortran) to acquire data, transfer to mag-tape as well as to format, and display the data. After the LC run is over, USER SERVICE ROUTINES and assembly coding is used to rewrite the directory area of the OPERATING SYSTEM (OS-8), so that access to the data may be had by using conventional keyboard or USR assembler calls. An overview schematic of the soft-

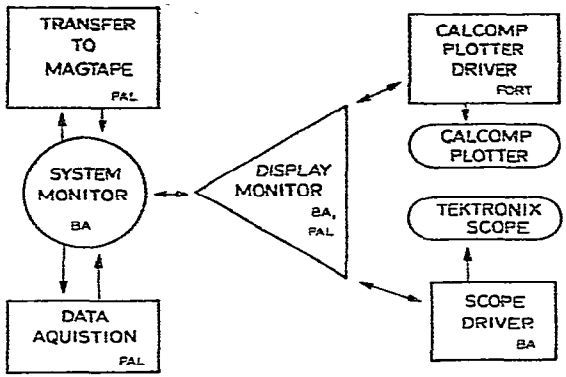

Fig. 13. Overview of computer system data flow and display.

ware support is shown in Fig. 13. A flow-chart for the shortest of the ten software programs is shown in Fig. 14.

I/O Display. During the 60-h LC run, a large amount of data (approximately 2.5 M words) is acquired that requires display in standard spectral and chromatographic format. During an LC run, the total absorbance chromatogram (TAC) is plotted out on a *Y/t* plotter associated with the system. This is the normal LC plot of response *vs.* time that is typical of single-wavelength monitors. The post-run operations include the following:

(1) Plotting of the absorbance at any single wavelength, or continuous band of wavelengths, or a selected group of wavelengths *vs.* time. A digital incremental plotter is used to provide the resolution and labeling required for documentation purposes. (absorbance band chromatogram, ABC)

(2) Listing of absorption peaks and times on the system terminal so that the technician can determine the elution time of a component for preparative purposes.

(3) Present an oscilliscope display of any given spectrum.

(4) Dumping of the data to industry compatible tape for storage, or transfer to a larger computer for full spectral display purposes or library search and matching of catalogued spectra.

APPLICATION

Pathological effects (mice)

ENS has several effects on the mouse bladder epithelium (C57 female, 12 weeks). A single oral dose (5–160 mg/kg) induces epithelial hyperplasia of the bladder in mice, whereas prolonged dietary administration (0.01 %, 8 weeks) of ENS produces a greater degree of epithelial hyperplasia and, frequently, bladder tumors at 30 weeks[29–31]. ENS, initially, causes a violent proliferative epithelial response which later settles into a chronic phase, in which cell tumor varies from animal to animal and site to site within the same bladder.

The sulfonamide group appears to be essential to the activity of the molecule due to the results of recent studies on sulfonyl and sulfonamide groups[30]. Maximum activity was found when the sulfonamide group was attached to an aromatic system

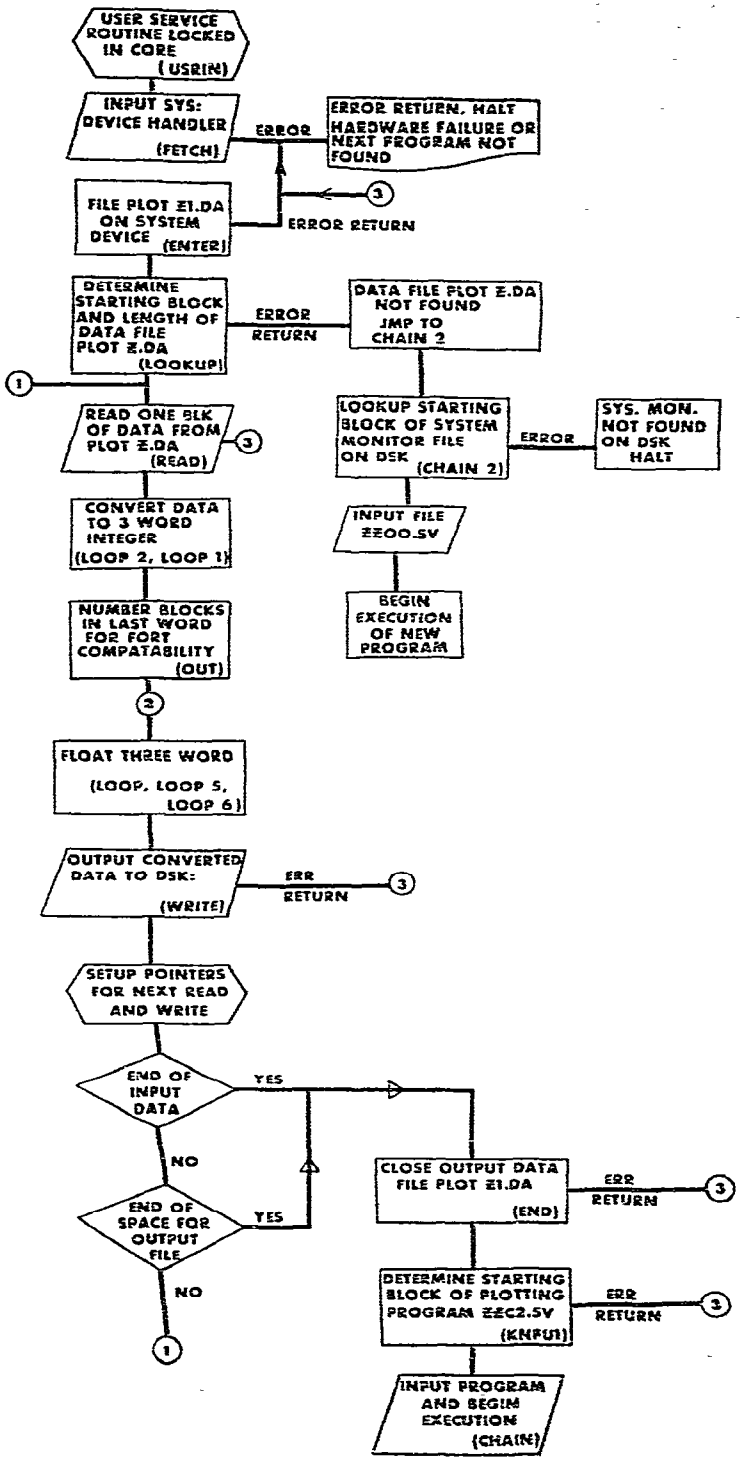

Fig. 14. Software program for binary to 3-word floating point convertor.

(benzene or naphthalene) containing an alkylsulfonyl or sulfonamide group. These implications of a structure–activity relationship have a bearing on the non-nutritive artificial sweeteners[29].

^{14}C-Labeled ENS metabolites

Presently, the metabolism of ENS in mice strains has not been fully determined. In the current series of studies, female BALB/C mice (20 weeks) were each fed 1.05 μCi of ^{14}C-labeled ENS (sp. act. 11 μCi/μmole). The urine was collected over a 24-h period in special metabolism cages. The pooled urine was filtered through a Millipore filter (0.2 μm) before chromatography. One hundred microliters of filtered urine were injected onto the 150 cm × 1/8 in. O.D. Aminex A-27 anion-exchange column and eluted with buffer gradient during the 55-h period. The separation was conducted under the following conditions: 0.1 ml/min flow-rate, 50° (isothermal), hyperbolic descending pH (8 → 4.40) over the first 5 h, ascending buffer gradients 0.1–6 *M* ammonium acetate–acetic acid over a 0–40 h period, holding 6 *M* buffer constant during a 40–55 h period. Fractions were taken every 10 min during the 50-h elution period. Individual ^{14}C-containing fractions were counted by a Nuclear-Chicago Mark II liquid scintillation instrument equipped with a Model PDS/3 data reduction system. The 1-ml fractions were added to a vial containing 12 ml of PCS solubilizer (Amersham-Searle, Arlington Heights, Ill., U.S.A.) and counted for 2 min. A plot of the count-rate data (dpm) *vs.* retention time for each 10-min fraction having significant dpm (>50) is shown in Fig. 3 (cross-hatch). The individual metabolites are shown at retention times of 26.5, 31.0, 35.5, 43.3, and 53.0 h. These accounted for 96% of the total measured radioactivity in the 100-μl urine sample.

LC–UV display

Work is continuing on improving the computer-driven Cal-Comp plotter display of both the total absorbance chromatogram and the absorbance band chromatogram. A recent example of the spectral output for both ENS (t_R = 31.0 h) and a suspected sulfonate conjugate (t_R = 43.3 h) is shown in Figs. 15 and 16, respectively.

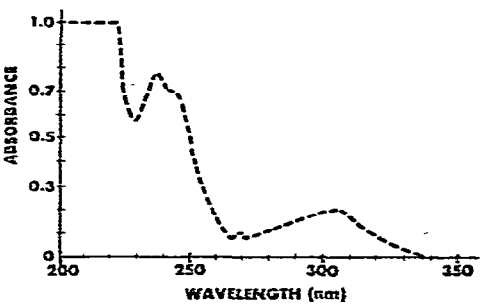

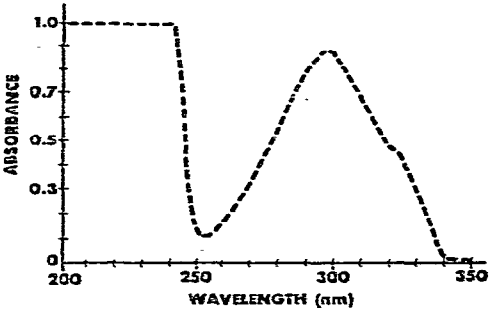

Fig. 15. Illustration of UV spectra (200–350 nm) of ENS from the Reticon spectrometer.

Fig. 16. Illustration of UV spectra (200–350 nm) of ENS metabolite from the Reticon spectrometer.

DISCUSSION

Our interest in the computerized LC–UV system is two-fold. First, the generation of a UV-spectral data base of urinary components (human and selected animal) associated with normal and pathological states with subsequent computer retrieval and matching is required for profiling of various in-born errors of metabolism. The acquisition of this data bank would aid immensely in the selection of UV spectral "windows" or binary descriptors for utilization in urinary profile development of specific human pathological states via computer pattern recognition techniques. The second purpose is the general utilization of the system for rapid UV data characterization of toxic chemical agents and their metabolites in urine. As shown by the current system, computer data manipulation can certainly enhance both the detection levels of components as well as aid in the chromatographic resolution of compounds.

LC has been hindered by the lack of a universal detector, and, consequently, no equivalent for the GC–MS system has yet been described. In the present work, we have begun to demonstrate the utility of a computerized LC–UV system for the rapid UV data acquisition and identification of various toxic chemical agents and their metabolites. Computer retrieval and display of selected UV spectra upon completion of an LC run saves many hours of tedious collection of many hundreds of fractions and transfer to a UV spectrometer. The added advantage of the capability to re-run the entire LC at a wavelength specific for the chemical toxicant or its metabolites under study enables its rapid location in the chromatogram for further spectroscopic study.

At this stage in the development, we have not "fine tuned" the system for maximum detectability. However, the spectrometer system has demonstrated increased sensitivity over single band monitoring by virtue of its computerized signal integration routine. Enhanced sensitivity will enable several improvements in LC column technology. Although the capacities of conventional resins are several hundredfold greater than those of pellicular resins, the improved sensitivity will enable lower sample loadings along with increased resolution with the concomitant use of pellicular resins for urinary metabolite identification and screening.

Future data manipulations for enhanced spectral presentation will include: (a) the use of ratios at two selected wavelengths for determination of peak homogeneity, (b) spectral base-line or background subtraction technique via computer routine, (c) peak de-convolution for improved resolution, and (d) on-line quantitative analysis.

ACKNOWLEDGEMENTS

The mini-computerized spectrometer unit was developed by the Instrumentation and Computer Interfacing Group, Department of Chemistry, Virginia Polytechnic Institute and State University and the National Center for Toxicological Research under Contract No. 222-75-2047(c). The mouse urine containing the ^{14}C-labeled ENS and metabolites was kindly supplied by Dr. James Stanley, Molecular Biology Division, National Center for Toxicological Research.

APPENDIX I —CALCULATION OF PHOTON RATE, REFERENCE BEAM RATE, SATURATION EXPOSURE, DYNAMIC RANGE, AND SAMPLE BEAM DETECTABILITY

Light source

From the spectral irradiance curve given in Fig. 4, $S_1 = 0.28\ \mu W/cm^2 \cdot nm$, and extrapolating to a 40.3 cm^2 mirror at 12.44 cm from the source, the total energy striking source mirror, E_m, is

$$E_m = \left(\frac{50}{12.44}\right)^2 (0.28)\,(10^{-6})\,(250)\,(40.3) = 0.114\ \text{W (250 nm)}$$

and

$$E_2 - E_1 = h\nu = 8 \times 10^{-12}\ \text{ergs/photon}$$

where the number of photons/W·sec is given by

$$\frac{1}{8 \times 10^{-12}} \frac{1}{10^{-7}} = 1.25 \times 10^{18}\ \text{photons/W·sec (at 250 nm)}$$

or

N = total photon flux at mirror (at 250 nm)

$$N = (0.114)\,(1.25 \times 10^{18}) = 1.42 \times 10^{17}\ \text{photons/sec (at 250 nm)}$$

The photon loss to entrance of fiber optics is approximated by the area ratios of image to fiber end

$$\frac{0.9 \times 1.5}{0.9 \times 4.0} = 0.38$$

The total number of photons/sec entering the fiber optics, assuming no scattering loss upon entrance,

$$N_1 = 0.38 \times 1.42 \times 10^{17}$$
$$= 5.39 \times 10^{16}\ \text{photons/sec}$$

The fiber optics are split into two beams, or

$$N_2 = 2.70 \times 10^{16}\ \text{photons/sec}$$

Assume a 50% loss through the fiber optics

$$N_3 = 1.35 \times 10^{16}\ \text{photons/sec}$$

These are the number of photons/sec at 250 nm presented to each of the reference and sample beams.

Reference beam

Assume 0.6 *M* acetic acid–acetate buffer (pH 4.4) and at 250 nm, the measured

absorbance is 0.015 (1 cm path length). The number of photons/sec which exit from the flow cell are

$$\frac{1}{2.3} \ln \frac{I_0}{I} = A, \text{ where } I_0 = N_3 = 1.4 \times 10^{16}$$

Solving for I

$$I = 1.3533 \times 10^{16} \text{ photons/sec}$$

Assume 50% loss through exit fiber optics to grating, or

$$I = 6.72 \times 10^{15} \text{ photons/sec at 250 nm}$$

Assume 50% energy transfer through grating and divergence loss proportional to area ratios [(pixel area)/(light beam area) = 0.0274]

$$I = (0.0137)(6.72 \times 15^{15})$$
$$= 9.135 \times 10^{13} \text{ photons/sec}$$

Saturation exposure (SE)

Given as 0.27 μW·sec/cm^2 (ref. 32) but the area of a single pixel is

$$A = 2.11 \times 10^{-4} \text{ cm}^2$$

or

$$SE_{CH} = 5.67 \times 10^{-5} \mu\text{W} \cdot \text{sec}$$
$$= 5.67 \times 10^{-5} \times 1.25 \times 10^{18} \times 10^{-6}$$
$$= 7.09 \times 10^{7} \text{ photons (at 250 nm)}$$

Noise per channel (NE)[32]

Given as 6.9×10^{-6} μW·sec/cm^2 at 30° then

$$NE_{CH} = 6.9 \times 10^{-6} \times 2.1 \times 10^{-4}$$
$$= 1.45 \times 10^{-9} \times 1.25 \times 10^{18} \times 10^{-6}$$
$$= 1.8 \times 10^{3} \text{ photons}$$

Dynamic range

Defined as maximum signal at saturation to the noise signal both measured at a fixed pixel

$$DR = \frac{SE_{CH}}{NE_{CH}}$$
$$= \frac{7.09 \times 10^{7}}{1.8 \times 10^{3}}$$
$$\approx 4 \times 10^{4} \text{ at } 30°$$

(By cooling to −30°, the DR may improve by a factor of 10.)

Sample beam

From previous calculation, $I_0 = 1.40 \times 10^{16}$ photons/sec at 250 nm, assume a guanosine concentration of 10^{-9} g/25 μl mouse urine (BALB/C); for guanosine

$$\varepsilon_{250} = 11{,}050 \text{ l/mole·cm (mol. wt. = 283)}$$

LC peak width = 3 min (estimated for 10^{-9} g); flow-rate = 0.1 ml/min; $V_R = 0.3$ ml; assume a true Gaussian peak shape, where $W = 10^{-9}$ g solution of

$$C(V) = \frac{W}{\sqrt{2\pi}\sigma} \int_{V_1}^{V_2} e^{\frac{-(V-V_0)^2}{2\sigma^2}} dv \qquad \text{(see Appendix II)}$$

Yields

$W_1 = 2.40 \times 10^{-10}$ g, or, the concentration in the light beam, $C_1 = 2.68 \times 10^{-8}$ moles/l.

Then

$$\text{Total absorption} = A_{\text{buffer}} + A_{\text{guan.}} \text{ (at 250 nm)}$$

or

$$\frac{1}{2.3} \ln \frac{I_0}{I} = 0.015 + a \cdot b \cdot c$$

where

$$I = 1.40 \times 10^{16},\ a = 1 \text{ cm},\ b = 11{,}050, \text{ and } c = 2.68 \times 10^{-8}.$$

Substituting gives

$$37.1778 - \ln I = 0.0352$$

$$I = 1.36 \times 10^{16} \text{ photons/sec}$$

Correcting for loss through exit fiber-optics and grating divergence loss (0.0068): $I = 9.192 \times 10^{13}$ photons/sec. The differential signal developed between the reference and sample detectors will be the net photons/sec times the photodiode sensitivity

$$dI_{\text{det.}} = (9.192 - 9.135)\ 10^{13} \text{ photons/sec}$$

$$= 5.7 \times 10^{11} \text{ photons/sec}$$

or

$$S_{\text{det.}} = \frac{(5.7 \times 10^{11})\,(8 \times 10^{-12})\,(10^{-7})\,(10^{6})\,(12 \times 10^{-12})}{2.2 \times 10^{-4}} = 5.2 \times 10^{-9} \text{ A}$$

APPENDIX II —SOLUTION OF GAUSSIAN CURVE FOR CONCENTRATION OF GUANOSINE IN 0.030-ml DETECTOR CELL

See Fig. 17 for details and peak measurements. V_0 = Retention volume of guanosine; $V_b - V_a = 0.030$ ml; $V_2 - V_1 = 0.3$ ml; $W = 10^{-9}$ g guanosine. The curve is of the general form

$$C(V) = \frac{W}{\sqrt{2\pi}\sigma} \exp \frac{-(V - V_0)^2}{2\sigma^2}$$

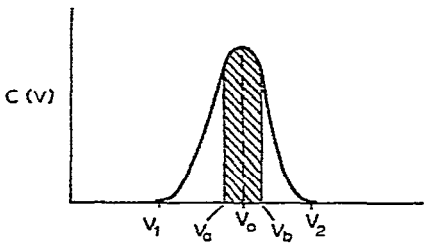

Fig. 17. LC Gaussian peak shape for guanosine.

Let $V_a = V_0 - \bigtriangledown$ and $V_b = V_0 + \bigtriangledown$ for the area

$$A_T = \int_{V_a}^{V_b} C(V)\mathrm{d}v$$

Because the area in the cross-hatched region is symmetrical about V_0, we simplify

$$A_1 = 2\int_{V_a}^{V_b} C(V)\mathrm{d}v$$

The function, F(x) is a cumulative probability function of a uniform normal distribution and has been extensively tabulated, or

$$\mathrm{F}(x) = \frac{1}{\sqrt{2\pi}} \int_{-\infty}^{x} \mathrm{e}^{\frac{-t^2}{2}}\,\mathrm{d}t$$

By making the transformation, $t = (V - V_0)/\sigma$, then $t = \mathrm{d}V/\sigma$.
So

$$\int_{-\infty}^{V'} C(V)\mathrm{d}v = WF(x')$$

then

$$A = 2\int_{V_a}^{V_b} C(V)\mathrm{d}v = 2\left[\int_{-\infty}^{V_b} C(V)\mathrm{d}v - \int_{-\infty}^{V_0} C(V)\mathrm{d}v\right]$$

$$= 2\,[W\mathrm{F}(X_b) - W\mathrm{F}\,(0)]$$
$$= 2\,W\,[\mathrm{F}\,(X_b) - 0.5]$$

For the LC curve, σ can be approximated as follows:

$$\sigma = \frac{V_2 - V_1}{6} = 0.5 \text{ ml}$$

then $x_b = 6\nabla/(V_2 - V_1)$
where $\nabla = 0.015$ and W and $V_2 - V_1$ have been given previously.
Thus

$$A = 2 \times 10^{-9} \left[\frac{F(6 \times 0.015)}{0.3} - 0.5\right]$$

$$= 2 \times 10^{-9} [F(0.3) - 0.5]$$
$$= 2 \times 10^{-9} (0.6179 - 0.5)$$
$$= 2.36 \times 10^{-10} \text{ g}$$

APPENDIX III —COMPARISON OF THE LINEAR PHOTODIODE ARRAY (512 PIXELS) UTILIZING SINGLE PIXEL TO THE PHOTOMULTIPLIER[33,34]

For the Reticon

$$\left(\frac{S}{N}\right)_{CH} = \frac{N_p Q_v T_e}{N_n N_f}$$

where

N_p = input photons/sec (= 10^4)
Q_v = quantum efficiency at specified wavelength (0.32 at 250 nm)
T_e = integration or dwell time per channel (1 sec)
N_n = noise (electrons/frame) (= 770)
N_f = number of frames (= 1)

$$\left(\frac{S}{N}\right)_{CH} = \frac{(10^4)\,(0.32)\,(1)}{(770)\,(1)} = \frac{32}{7.7} = 4.1:1$$

For photomultiplier, single-wavelength sensing for grating (250 nm, 1 nm bandwidth)

$$\left(\frac{S}{N}\right)_{CH} = \frac{N_p Q_p GK}{N_{PM}}$$

where

N_p = input photons/sec (= 10^4)
Q_p = quantum efficiency (0.1 at 250 nm)
G = gain ($\approx 10^6$)
K = C/electro-static units (= 1.6×10^{-19})
N_{PM} = photomultiplier dark current noise ($\approx 6 \times 10^{-12}$ A)

$$\left(\frac{S}{N}\right)_{PM} = \frac{(10^4)\,(0.1)\,(10^6)\,(1.6 \times 10^{-19})}{6 \times 10^{-12}} = \frac{16}{6} = 26:1$$

REFERENCES

1 K. Callmer and O. Nilsson, *Chromatographia*, 6 (1973) 517.
2 C. J. O. R. Morris, *Lab. Pract.*, 23 (1974) 513.
3 H. Veening, *J. Chem. Educ.*, 50 (1973) A481.
4 M. Krejci, *Chem. Listy*, 57 (1973) 843.
5 E. S. Watson, *Ger. Offen. Pat.*, 2,258,208, 7 June (1973).
6 E. D. Pellizzari and C. M. Sparacino, *Anal. Chem.*, 45 (1973) 378.
7 D. R. Baker, R. C. Williams and J. C. Steichen, *J. Chromatogr. Sci.*, 12 (1974) 499.
8 A. Sonnenschein, *Anal. Instrum.*, 12 (1974) 123.
9 J. Koszewski, A. Bylina, D. Sybilska and Z. R. Gravowski, *Brit. Pat.*, 1,339,475, 5 December, 1973.
10 J. C. Steichen, *J. Chromatogr.*, 104 (1975) 39.
11 N. P. Dimov, *Dokl. Bolg. Akad. Nauk*, 27 (1974) 1407.
12 M. S. Denton, T. P. DeAngelis, A. M. Yacynych, W. R. Heineman and T. W. Gilbert, *Anal. Chem.*, 48 (1976) 20.
13 B. Sauer, *GIT Fachz. Lab.*, 17 (1973) 1152.
14 A. Bylina, D. Sybilska, Z. R. Grabowski and J. Koszewski, *J. Chromatogr.*, 83 (1973) 357.
15 M. J. Milano and H. L. Pardue, *Anal. Chem.*, 47 (1975) 25.
16 H. L. Pardue, A. E. McDowell, D. M. Fast and M. J. Milano, *Clin. Chem.*, 21 (1975) 1192.
17 Y. Talmi, *Anal. Chem.*, 47 (1975) 659A.
18 Y. Talmi, *Anal. Chem.*, 47 (1975) 687A.
19 R. Dessy, W. G. Nunn, W. D. Reynolds and C. A. Titus, *Pittsburgh Conf. Anal. Chem. & Appl. Spectrosc., 27th, March 1976*, paper No. 375.
20 A. G. Marshall and M. B. Comisarow, *Anal. Chem.*, 47 (1975) 491A.
21 F. W. Plankey, T. H. Glenn, L. P. Hart and J. D. Winefordner, *Anal. Chem.*, 46 (1974) 1006.
22 B. L. Karger, M. Martin and G. Guiochon, *Anal. Chem.*, 46 (1974) 1640.
23 M. W. Anders and J. P. Latorre, *Anal. Chem.*, 42 (1970) 1430.
24 M. W. Anders and J. P. Latorre, *J. Chromatogr.*, 55 (1971) 409.
25 J. E. Mrochek, S. Katz, W. H. Cristie and S. R. Dinsmore, *Clin. Chem.*, 20 (1974) 1086.
26 J. X. Khym, *Analytical Ion-Exchange Procedures in Chemistry and Biology*, Prentice-Hall, Englewood Cliffs, N.J., 1974.
27 P. R. Brown, *High-Pressure Liquid Chromatography; Biochemical and Biomedical Applications*, Academic Press, New York, 1973.
28 C. D. Scott, *Sep. Purif. Methods*, 3 (1974) 263.
29 A. Flaks, J. M. Hamilton and D. B. Clayson, *J. Nat. Cancer Inst.*, 51 (1973) 2007.
30 D. B. Clayson, A. J. Bedford and R. Turner, *Chem.-Biol. Interactions*, 6 (1973) 107.
31 P. E. Levi, J. C. Knowles, D. M. Cowen, M. Wood and E. H. Cooper, *J. Nat. Cancer Inst.*, 46 (1971) 337.
32 R. R. Buss (Reticon Corp., 910 Benicia Avenue, Sunnyvale, Calif.), personal communication.
33 Y. Talmi, R. Crosmum and N. M. Larson, *Anal. Chem.*, 48 (1976) 326.
34 G. G. Olson, *Amer. Lab.*, February (1972) 69.